# Ligand–Substrate Communication in Group 4 Aminopyridinato Complexes

**Markus Oberthür, Gerhard Hillebrand, Perdita Arndt, and Rhett Kempe***

Max-Planck-Gesellschaft, Arbeitsgruppe "Komplexkatalyse" an der Universität Rostock, Buchbinderstraße 5–6, D-18055 Rostock, Germany

Received November 11, 1996

**Keywords:** Agostic interactions / Ligand effects / Titanium / Zirconium / Aminopyridinato ligands

Tris(aminopyridinato) zirconium and *ansa*-aminopyridinato titanium complexes have been synthesized. The reaction of (TMS–APy)$_3$–Zr–Cl (4-methyl-2-trimethylsilyl-aminopyridine = TMS–APy–H) with trimethylsilylbutadiynyl lithium generated in situ affords (TMS–APy)$_3$–Zr–C≡C–C≡C–TMS (**1**). (TMS–APy)$_3$–Zr–Cl reacts with lithium dimethylamide and leads to (TMS–APy)$_3$–Zr–NMe$_2$ (**2**). Compound **2** shows an agostic interaction of the dimethylamido moiety. The reaction of Ti(NMe$_2$)$_4$ with silox(APy–H)$_2$[1,3-di(4'-picolin-2'-yl-amino)-1,1,3,3-tetraisopropyldisiloxane = silox(APy–H)$_2$] gives rise to silox(APy)$_2$–Ti–(NMe$_2$)$_2$ (**3**). Complex **3** reacts with ε-caprolactam to form a caprolactamato complex (**4**). X-ray crystal structure analyses of **1**, **2**, **3** and **4** are reported. The complexes **1**, **2**, **3** and **4** may be considered to be strained donor-functionalized amido(metal) complexes due to the $\eta^2$ binding mode of the aminopyridinato ligands. An adaptation of the binding mode of the ligand cores, TMS–APy and silox(APy)$_2$, to meet the requirements of the ancillary coordinated substrates is observed. Thus, aminopyridinato complexes seem to be valuable model compounds for investigations of ligand–substrate communications in early transition metal chemistry.

## Introduction

Ligand-substrate communication (steric repulsion between a ligand core and an ancillary coordinated substrate as well as electronic interactions of both via the metal center) plays a fundamental part in all metal-mediated transformation reactions, especially in catalysis. Whereas the design of a reactive metal center is well understood in many cases[1], little is known about the opposite influence, how substrate binding changes the coordination mode of a certain ligand core. We are currently investigating the use of aminopyridinato[2,3,4] (see A in Scheme 1) and *ansa*-aminopyridinato transition metal complexes[5] (see B in Scheme 1) to stabilize unusual coordination geometries and with regard to catalytic applications[5,6].

Scheme 1. Schematic representation of aminopyridinato (**A**) and *ansa*-aminopyridinato (**B**) complexes (M = early transition metal)

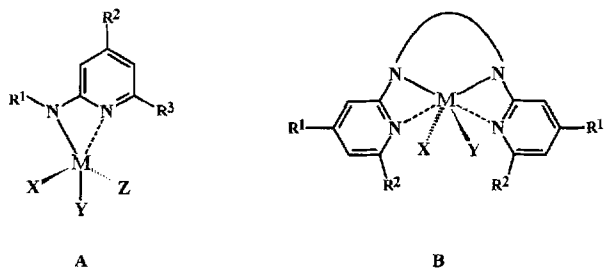

**A** **B**

Due to the high flexibility of such ligands in their binding mode (see Scheme 2) the corresponding metal complexes may act as model systems for studying ligand–substrate communication, because the ligands are sensitive to the steric and electronic needs of the ancillary coordinated substrates.

Scheme 2. Schematic representation of the binding mode of aminopyridinato ligands (M = early transition metal)

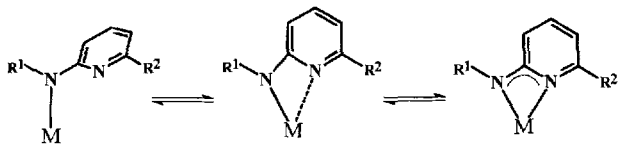

In this paper we report the synthesis and structure of a σ-butadiynyl– and a dimethylamido–zirconium complex. Both compounds contain a tris-aminopyridinato ligand core. An agostic interaction of the dimethylamido moiety with the zirconium center is introduced in the latter complex. Furthermore we report on *ansa*-aminopyridinato–titanium complexes that accommodate dimethylamido and ε-caprolactamato moieties. The binding mode of both aminopyridinato ligand cores is discussed with respect to the ancillary coordinated substrates.

## Results and Discussion

### Tris(aminopyridinato)zirconium Complexes

The reaction of MeLi with bis(trimethylsilyl)butadiyne gives rise to trimethylsilylbutadiynyl lithium[7]. One equiv. of the lithium salt reacts with (TMS–APy)$_3$Zr–Cl[4] (4-methyl-2-trimethylsilylaminopyridine = TMS–APyH) to afford (TMS–APy)$_3$Zr–C≡C–C≡C–TMS (**1**) according to eq. 1 in a moderate yield (24%) as a pale yellow crystalline material.

The $^1$H-NMR spectrum of **1** shows the single signal set of the TMS–APy ligand and the TMS signal of the butadiynyl moiety in the expected 3:1 ratio. A low-temperature

  0009–2940/97/0606–0789 $ 17.50+.50/0 

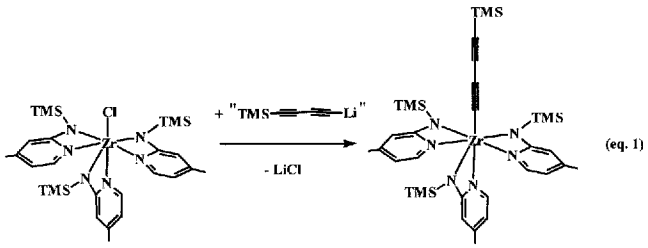


1

NMR investigation did not reveal any splitting of the signal sets, thus a threefold symmetry is proposed as the dominating arrangement in solution. Since structural data of zirconium complexes that contain a "free" σ-bound butadiynyl moiety are not available (according to a search of the Cambridge Crystallographic database), an X-ray analysis of **1** was carried out. Suitable crystals were obtained by recrystallization of **1** from hexane at −30 °C. A perspective ORTEP drawing of the molecular structure of **1** is shown in Figure 1 along with selected bond distances and angles. Some important crystallographic features are summarized in Table 1. The structure analysis confirms the threefold symmetry of the ligand core and shows a propeller-like arrangement of the three aminopyridinato ligands as observed for similar complexes. The bond parameters of the aminopyridinato ligands are in the expected range[4,8]. The averaged $Zr-N_{amido}$ bond length of **1** (2.19 Å) is approximately 0.1 Å longer than the usual zirconium amido bond length [2.11(1) Å][4] and indicates a weak metal−amido bond. The averaged $Zr-N_{pyridine}$ bond length of **1** (2.30 Å) is approximately 0.1 Å shorter than such bonds normally [2.39(1) Å][4], and seems to gain stability from the metal−amido bond. The $Zr-C_{butadiynyl}$ bond length [2.254(6) Å] is very well in accordance with such distances normally [2.237(13) Å][9]. The butadiynyl moiety deviates from linearity by up to 5.5°.

The reaction of $(TMS-APy)_3ZrCl$ with $LiNMe_2$ yields $(TMS-APy)_4Zr$, an eight-coordinated amido zirconium complex (Scheme 3).

Recently the synthesis and structure of a related hafnium complex $(Ph-APy)_4Hf$ (Ph−APy−H = anilinopyridine) was achieved[10]. The original intention of reaction 2 was to prepare $(TMS-APy)_3Zr-NMe_2$ (**2**). By following the course of the reaction using $^1$H-NMR spectroscopy, an intermediate was detected. This contained a dimethylamido moiety and the aminopyridinato ligands in a ratio of 1:3. Attempts to isolate **2** failed. The reaction of 3 equiv. of TMS−APy−H with one equiv. of $Zr(NMe_2)_4$ in ether at −78 °C leads to complex **2** (see eq. 2) in 92% yield. The reaction proceeds smoothly by amine elimination if the temperature is kept at −78 °C until **2** is isolated. **2** crystallizes as pale yellow, almost colorless, prisms.

Low-temperature NMR investigation of complex **2** indicates a splitting of the single signal set of the aminopyridinato ligands but no splitting at all for the dimethylamido moiety down to 190 K. Thus an asymmetric arrangement of the trisaminopyridinato ligand core is assumed. The single crystal X-ray structure analysis of **2** establishes its monomeric structure as shown in Figure 2, which includes principal bond distances and angles. Crystallographic data are listed in Table 1. Although the solid state structure of **1** is highly symmetric, **2** shows asymmetry in the arrangement of the aminopyridinato ligands and an unusual binding mode of the dimethylamido moiety. The geometric param-

Figure 1. Structural diagram of **1** with labeling scheme; non-hydrogen atoms are represented as thermal ellipsoids at the 30% probability level; selected bond lengths (Å) and angles (°): C(16)−Zr 2.254(6), N(1)−Zr 2.182(4), N(2)−Zr 2.294(4), N(3)−Zr 2.183(4), N(4)−Zr 2.291(4), N(5)−Zr 2.209(4), N(6)−Zr 2.325(4), N(2)−C(1)−N(1) 110.0(5), N(4)−C(6)−N(3) 109.1(5), N(6)−C(11)−N(5) 111.8(5), C(16)−C(17)−C(18) 174.5(7), C(19)−C(18)−C(17) 178.0(7), C(18)−C(19)−Si(4) 175.4(6)

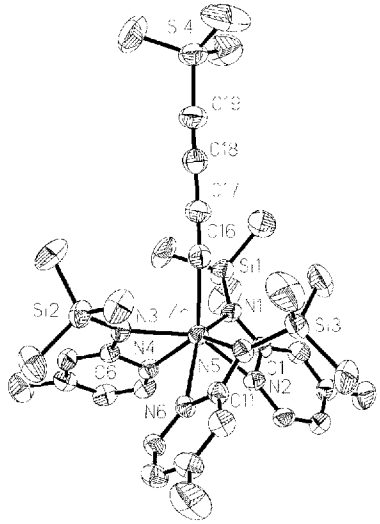


Table 1. Crystallographic data for **1**, **2**, **3** and **4**

| | **1** | **2** | **3** | **4** |
|---|---|---|---|---|
| formula | $C_{34}H_{54}N_6Si_4Zr$ | $C_{29}H_{51}N_7Si_3Zr$ | $C_{28}H_{52}N_6OSi_2Ti$ | $C_{32}H_{56}N_6O_2Si_2T$ |
| mol. mass | 750.4 | 673.3 | 592.8 | 660.9 |
| cryst. color | colorless | colorless | red | brown |
| cryst. descript | prism | prism | prism | prism |
| cryst. size (mm) | 0.3 × 0.15 × 0.15 | 0.5 × 0.4 × 0.3 | 0.5 × 0.4 × 0.4 | 0.5 × 0.4 × 0.3 |
| cryst. system | monoclinic | triclinic | monoclinic | monoclinic |
| space group | $P2_1/c$ | P-1 | $P2_1/c$ | $P2_1/c$ |
| lattice constants | | | | |
| $a$ (Å) | 14.000(2) | 10.921(1) | 11.191(1) | 11.188(2) |
| $b$ (Å) | 12.783(2) | 12.530(1) | 10.357(2) | 17.517(3) |
| $c$ (Å) | 25.849(4) | 15.639(1) | 30.071(3) | 19.143(3) |
| α (deg) | | 78.82(1) | | |
| β (deg) | 104.96(1) | 82.546(8) | 93.258(8) | 91.07(1) |
| γ (deg) | | 76.109(9) | | |
| $Z$ | 4 | 2 | 4 | 4 |
| temp. (K) | 293 | 293 | 293 | 293 |
| $\mu$ ($mm^{-1}$) | 0.381 | 0.384 | 0.343 | 0.327 |
| abs. cor. | no | Ψ scan | Ψ scan | no |
| transm.(%) min./max. | | 93.5/100.0 | 93.6/99.6 | |
| θ range (deg) | 1.79–24.30 | 2.33–24.97 | 2.08–24.98 | 1.82–24.32 |
| larg. diff. (e $Å^{-3}$) peak / hole | 0.24/–0.39 | 1.65/–0.41 | 0.49/–0.40 | 0.46/–0.36 |
| rflns. (measd.) | 12888 | 7476 | 6230 | 11012 |
| rflns. (indep.) | 7050 | 7116 | 6110 | 5983 |
| $R$ (int) | 0.113 | 0.022 | 0.045 | 0.034 |
| rflns. (obsd.) $[I > 2\sigma(I)]$ | 2622 | 4750 | 3604 | 3962 |
| no. parameters | 407 | 370 | 343 | 388 |
| $R1$ $[I > 2\sigma(I)]$ | 0.044 | 0.068 | 0.069 | 0.044 |
| $wR2$ (all data) | 0.102 | 0.264 | 0.214 | 0.120 |

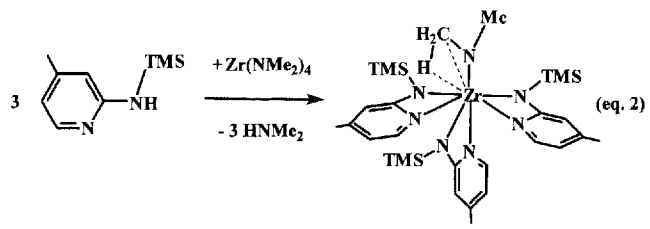


2

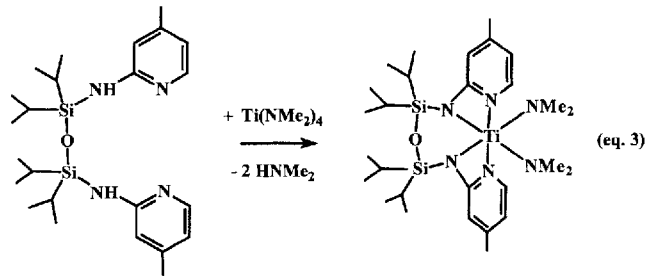


3

eters of the coordination of the latter are represented in Scheme 4.

Figure 2. Structural diagram of **2** with labeling scheme; non-hydrogen atoms are represented as thermal ellipsoids at the 30% probability level; selected bond lengths (Å) and angles (°): C(26)–N(6) 1.440(9), C(27)–N(6) 1.427(10), C(27)–Zr(1) 2.812(8), N(1)–Zr(1) 2.295(6), N(2)–Zr(1) 2.326(5), N(3)–Zr(1) 2.276(6), N(4)–Zr(1) 2.274(5), N(5)–Zr(1) 2.308(5), N(6)–Zr(1) 2.034(5), N(1)–C(10)–N(4) 110.7(6), N(7)–C(16)–N(2) 111.7(6), N(5)–C(21)–N(3) 110.9(6), Zr(1)–C(27)–HA27 133(6), Zr(1)–C(27)–HB27 120(5), HA27–C(27)–HB27 101(7Zr(1)–C(27)–HC27 76(4), HA27–C(27)–HC27 124(7)

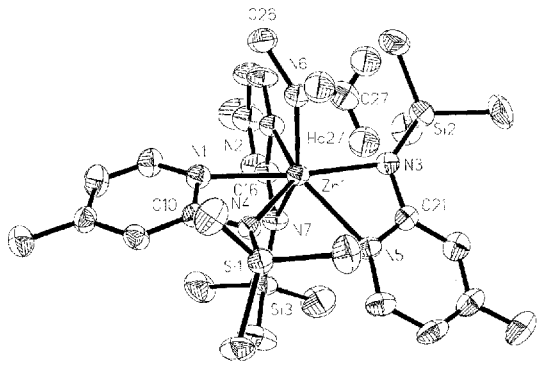


Scheme 3. Synthesis of $(TMS-APy)_4Zr$

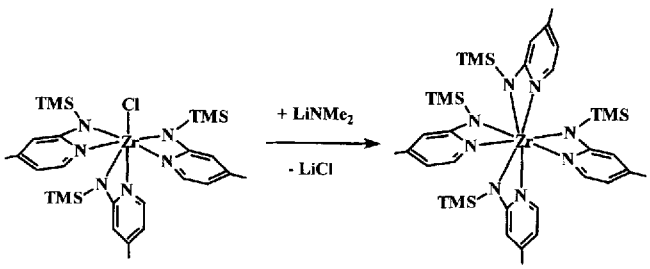


The solid state structure exhibits agostic interaction of the methyl groups of the dimethylamido moiety, although

Figure 3. Space-filling diagrams of **2**

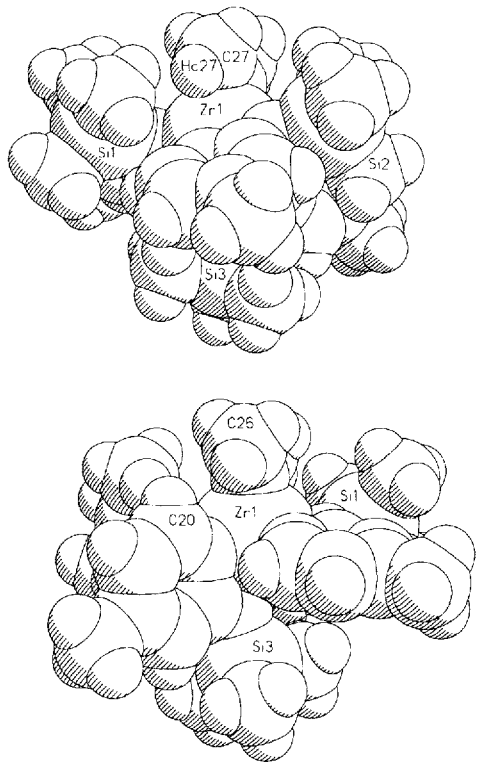


Scheme 4. Schematic representation of the agostic interaction of the dimethylamido ligand in **2** (distances [Å] and angles [°])

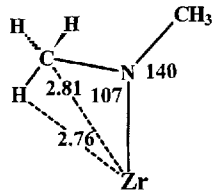


this could not be proved by NMR studies in solution. The explanation that packing effects may play the dominant role can be excluded. As seen from the space-filling diagram of **2** (Figure 3) the sterically demanding part of the ligand core does not force the dimethylamido moiety into its coordination mode. There is no example described among the published and structurally characterized dimethylamido–zirconium complexes that exhibits such an unusual binding mode. The recently determined structure of $Cp_2Zr(NMe_2)_2$[11] indicates a similar dimethylamido coordination as observed for **2**.

### (*ansa*-Aminopyridinato)titanium Complexes

The reaction of silox$(APy-H)_2$ with one equiv. $Ti(NMe_2)_4$ affords a red-brown crystalline sample of **3** in 91% yield according to eq. 3.

**3** is soluble in nonpolar solvents and can be recrystallized from ether. The $^1H$- and $^{13}C$-NMR spectra of **3** exhibit a sharp singlet for Me–Py and for dimethylamide. The isopropyl range exhibits only one signal set, a duplet and a septet, as expected for $C_2$ or $C_m$ symmetry in solution. No

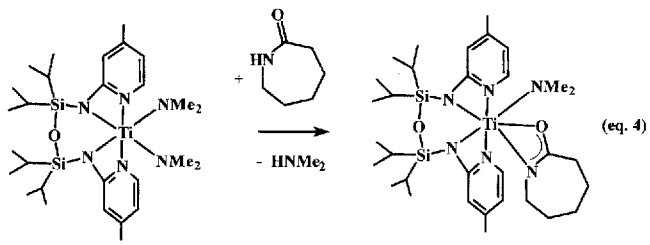


4

splitting of the signal sets could be detected by NMR spectroscopy. Suitable single crystals could be obtained after recrystallization of **3** in ether. A perspective ORTEP drawing of the molecular structure of **3** is shown in Figure 4 along with selected bond distances and angles. Some important crystallographic features are summarized in Table 1. The coordination geometry of **3** is best described as distorted octahedral. The equatorial plane is occupied by an amido moiety (N5), a strained $\eta^2$-bound aminopyridinato moiety (N1 and N2) and the amido nitrogen of the other aminopyridinato moiety (N3). The second pyridine (N4) is situated below this plane, with the second dimethylamido moiety above it. The amido nitrogen atoms N1, N5 and N6 have an almost planar geometry, as has been found in virtually all structurally characterized transition metal amido complexes[12]. The other amido nitrogen atom (N3) is a nonplanar exception to that rule. In order to accomplish the octahedral coordination geometry as is common for six-coordinated titanium $d^0$ complexes, the aminopyridinato ligand array in **3** has to be twisted. The different coordination modes of the two aminopyridinato parts of the chelating ligand are reflected also in the titanium–nitrogen bond parameters. The Ti1–N1 [2.181(4) Å] and Ti1–N2 [2.164(4) Å] bond lengths (in the equatorial plane) are almost equal and thus might be considered to be delocalized. Such a binding mode is observed for the related benzamidinato ligands[13]. Two different titanium–nitrogen bond lengths are observed for the other part of the aminopyridinato ligand ("out of plane"): Ti–N3 [2.070(4) Å] and Ti–N4 [2.226(4) Å]. The $Ti-N_{amido}$ distance (the former) is approximately 0.1 Å longer than the usual titanium–amido bond length [1.889(2) Å[3]], whereas the $Ti-N_{pyridine}$ distance (the latter) reflects a value almost identical to that normally observed for titanium–pyridine bonds [2.247 (7) Å[3]]. The coordination mode of the "out-of-plane" aminopyridinato moiety indicates the situation shown in Scheme 2 (middle formula) whereas the "in-plane" coordinated aminopyridinato moiety exhibits a delocalized binding mode (right formula).

The reaction of **3** with one equiv. of ε-caprolactam leads to complex **4** (see eq. 4), which can be obtained as a dark red crystalline material in 78% yield after recrystallization from ether. The $^1$H-NMR spectrum of **4** exhibits a single signal set of one aminopyridinato ligand, of one amido and one caprolactamato moiety. The results of an elemental analysis are consistent with the formulation of **4** as given in eq. 4. An X-ray crystal structure analysis was carried out

Figure 4. Structural diagram of **3** with labeling scheme; non-hydrogen atoms are represented as thermal ellipsoids at the 30% probability level; selected bond lengths (Å) and angles (°): N(1)–Ti(1) 2.181(4), N(2)–Ti(1) 2.164(4), N(3)–Ti(1) 2.070(4), N(4)–Ti(1) 2.226(4), N(5)–Ti(1) 1.923(4), N(6)–Ti(1) 1.920(4), N(2)–C(9)–N(1) 110.5(4), N(4)–C(16)–N(3) 110.8(4), Si(2)–O(1)–Si(1) 139.6(2)

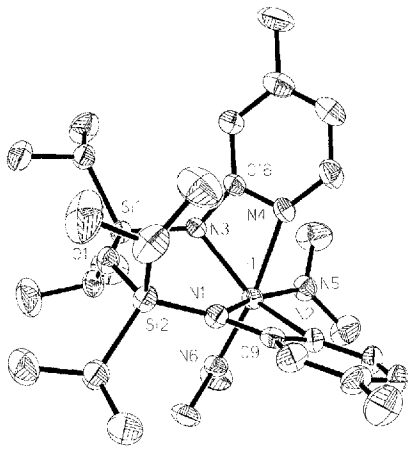


to explore the binding situation of the aminopyridinato ligand and the caprolactamato moiety. The activation of caprolactam by early transition metal complexes has rarely been described[14]. The single crystal X-ray structure analysis of **4** establishes its monomeric structure as that shown in Figure 5, which includes selected bond distances and angles. Crystallographic data are listed in Table 1. The coordination geometry is best described as distorted pentagonal bipyramidal. The *ansa*-aminopyridinato ligand occupying the equatorial plane is planar. The averaged nitrogen–titanium bond lengths ($Ti-N_{amido}$ 2.15 Å, $Ti-N_{pyridine}$ 2.18 Å) are almost equal, indicating a delocalized binding mode as shown in Scheme 2 (right formulation). The caprolactamato moiety binds in a strained $\eta^2$ fashion with similar Ti–N and Ti–O [N(6)–Ti(1) 2.139(2) Å, O(2)–Ti(1) 2.172(2) Å] and C–N and C–O bond lengths [C(6)–O(2) 1.297(4) Å, C(6)–N(6) 1.302(4) Å] in the Ti–N–C–O four-membered ring.

### Ligand-Substrate Communication

The propeller-like arrangement of the three aminopyridinato ligands in **1** may cause a kinetic stabilization. The sensitive zirconium–carbon bond is sterically shielded by the three bulky trimethylsilyl groups. This coordination mode seems to be favored with regard to electronic considerations[4,8] and is accomplished as long as the steric demand of the ancillary coordinated substrate does not dictate the arrangement of the aminopyridinato ligand core by its steric bulk. If the substrate is sterically demanding, like the dimethylamido moiety (see complex **2**), the aminopyridinato-coordinated metal center easily alters its coordination mode. This alteration is facilitated by the extraordinary flexibility of the ligand system. It opens up a large coordination site to provide space even for an agostic interaction of the methyl group of the dimethylamido moiety. Such an interaction has not previously been described. It is pro-

Figure 5. Structural diagram of **4** with labeling scheme; non-hydrogen atoms are represented as thermal ellipsoids at the 30% probability level; selected bond lengths (Å) and angles (°): N(1)–Ti(1) 2.146(2), N(2)–Ti(1) 2.186(2), N(3)–Ti(1) 2.141(2), N(4)–Ti(1) 2.181(2), N(5)–Ti(1) 1.892(2), N(6)–Ti(1) 2.139(2), O(2)–Ti(1) 2.172(2), N(2)–C(1)–N(1) 109.3(2), O(2)–C(6)–N(6) 114.6(3), N(4)–C(12)–N(3) 109.2(2), Si(1)–O(1)–Si(2) 140.86(12), N(6)–Ti(1)–O(2) 60.95(8)

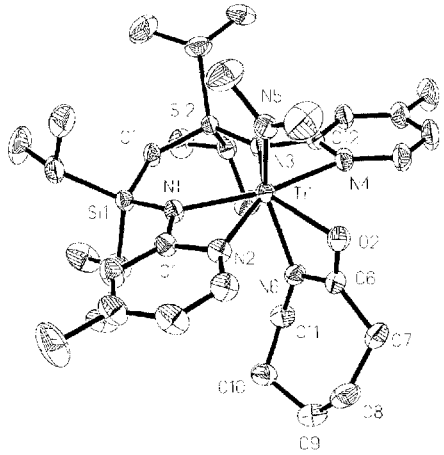


posed as an intermediate of the early transition metal catalyzed aminomethylation of nonactivated olefins[15]. An adaptation of the coordination mode of the ligand core can also be observed by comparing **3** and **4**. Complex **3** is a six-coordinated compound. To accomplish an octahedral coordination geometry the aminopyridinato ligand has to be twisted. Thus two different binding modes in the ligand core can be observed. To bind caprolactam the coordination number is raised from six to seven. The pyridine moiety situated "out of plane" in **3** is turned in-plane in the case of **4** to offer the additionally needed coordination site. Hence, the ligand becomes planar. In addition to the geometric rearrangement, the binding mode of the formerly "out-of-plane" ligand arm is switched to the delocalized form (almost equal Ti–N bond distances). Steric and electronic changes are necessary to meet the requirements of the caprolactamato moiety.

### Conclusion

A more general conclusion can be drawn from this study. Aminopyridinato ligands in group 4 metal complexes are characterized by an extraordinary flexibility in their binding mode. Due to the ability of the ligands to adapt themselves easily to different coordination modes, they meet perfectly the steric and electronic requirements of different substrates additionally coordinated to the metal center. Hence, complexes containing aminopyridinato ligands may act as model compounds for studying ligand–substrate communication and thus improving knowledge of interactions between a ligand core and substrates.

We thank Prof. *U. Rosenthal* for generous support and helpful discussions. Financial support by the *Max-Planck-Gesellschaft* and *Fonds der Chemischen Industrie* is gratefully acknowledged.

## Experimental Section

*General:* All operations were carried out under argon with standard Schlenk techniques. Prior to use solvents were freshly distilled from sodium tetraethylaluminate and stored under argon. Deuterated solvents were treated with sodium or sodium tetraethylaluminate, distilled and stored under argon. – Mass spectra: AMD 402. – NMR spectra: Bruker ARX 400. Chemical shifts were referenced to signals of the solvents used: [D$_8$]THF (β-CH$_2$: $\delta_H$ = 1.73, $\delta_C$ = 25.2) or C$_6$D$_6$ ($\delta_H$ = 7.16, $\delta_C$ = 128.0). – Melting points: sealed capillaries, Büchi 535 apparatus. – Elemental analyses: Leco CHNS-932 elemental analyzer. – X-ray diffraction data: STOE-IPDS or CAD4-MACH3 diffractometer using graphite-monochromated Mo-$K_\alpha$ radiation. The crystals were sealed inside capillaries. The structures were solved by direct methods (SHELXS-86[16]) and refined by full-matrix least-squares techniques against $F^2$ (SHELXL-93[17]). XP (SIEMENS Analytical X-ray Instruments, Inc.) was used for structure representations. Further details of the crystal structure investigations are available upon request from the Director of the Cambridge Crystallographic Data Centre, 12 Union Road, Cambridge CB21EZ (UK), on quoting the deposition number CSD-100112, the names of the authors, and the journal citation. The fairly large $wR^2$ values (all data) of compounds **2** and **3** are attributed to the poor diffraction behavior of the crystals, and the fact that in the case of weak reflections a conventional diffractometer scans for a significantly shorter time than an imaging plate is exposed for, and thus weak reflections are better considered in the latter case.

*Preparation of* **1**: To a solution of 1,4-bis(trimethylsilyl)buta-1,3-diyne (0.41 g, 2.10 mmol) in diethyl ether (30 ml) was added MeLi–LiBr complex (1.4 ml, 2.10 mmol; 1.5 M in Et$_2$O). After stirring the solution for 19 h at room temp. (TMS–APy)$_3$ZrCl[4] (1.40 g, 2.10 mmol) was added. Stirring was continued for 72 h and the color changed to green-brown. After complete removal of the solvents the remaining colorless crystalline solid was extracted with *n*-hexane (30 ml) and recrystallized at −30°C. Yield: 0.38 g (0.50 mmol, 24%) of colorless crystals. – $^1$H NMR ([C$_6$D$_6$]): δ = 7.30 (d, 3H, *J* = 5.5 Hz, 6-H), 6.21 (s, 3H, 3-H), 5.85 (d, 3H, *J* = 5.5 Hz, 5-H), 1.73 (s, 9H, Me), 0.47 (s, 27H, APy–SiMe$_3$), 0.09 (s, 9H, SiMe$_3$). – $^{13}$C NMR ([C$_6$D$_6$]): δ = 168.1 (C-2), 152.0 (C-4), 142.7 (C-6), 112.0, 111.9 (C-3, C-5), 143.6, 92.2, 90.4, 80.6 (alkyne-C), 21.6 (Me), 0.9 (APy–SiMe$_3$), 0.1 (SiMe$_3$). – $C_{34}H_{54}N_6Si_4Zr$ (750): calcd. C 54.42, H 7.25, N 11.20; found C 54.07, H 7.13, N 11.29.

*Preparation of* **2**: 4-Methyl-2-(trimethylsilylamino)pyridine (1.07 g, 5.96 mmol) was added slowly to a solution of Zr(NMe$_2$)$_4$ (530 mg, 1.99 mmol) in diethyl ether (20 ml) at −78°C. After stirring (1 h, −78°C) **2** was crystallized at −78°C. Crystallization was induced by product formation. The mother liquor was filtered off. Yield: 1.23 g (1.84 mmol, 92%) of colorless crystals. $^1$H NMR ([C$_6$D$_6$]): δ = 7.64 (d, 3H, *J* = 5.6 Hz, 6-H), 6.26 (s, 3H, 3-H), 5.92 (d, 3H, *J* = 5.6 Hz, 5-H), 3.17 (s, 6H, N–Me), 1.79 (s, 9H, APy–Me), 0.28 (s, 27H, SiMe$_3$). – $^{13}$C NMR ([C$_6$D$_6$]): δ = 171.5 (C-2), 150.3 (C-4), 143.4 (C-6), 112.9, 110.1 (C-3, C-5), 42.9 (N–Me), 21.5 (APy–Me), 1.6 (SiMe$_3$). – $C_{29}H_{51}N_7Si_3Zr$ (673): calcd. C 51.74, H 7.64, N 14.56; found C 51.32, H 7.34, N 13.65.

*Preparation of* **3**: Via a syringe, Ti(NMe$_2$)$_4$ (2.12 g, 9.46 mmol) was added to a stirred solution of silox(APy–H)$_2$[5] (4.33 g, 9.46 mmol) in diethyl ether (30 ml) at room temp. The dark red solution was stirred for 30 minutes, concentrated under reduced pressure to 15 ml and stored for 20 hours at −78°C. The mother liquor was decanted off, the crystals were collected and dried in vacuo. Yield: 5.11 g (8.64 mmol, 91%) of red-brown crystals. – $^1$H NMR (C$_6$D$_6$): δ = 7.45 (d, 2H, *J* = 5.4 Hz, 6-H), 6.30 (s, 2H, 3-H), 5.97 (m, 2H, 5-H), 3.34 (s, 12H, N–Me), 1.85 (s, 6H, APy–Me), 1.37–1.26 (m, 28H, *i*-Pr–Si). – $^{13}$C NMR (C$_6$D$_6$): δ = 168.5 (C-2), 150.1 (C-4),

142.4 (C-6), 113.7 (C-5), 112.0 (C-3), 48.3 (N−Me), 21.5 (APy−Me), 18.9, 18.7 (CH−Me), 16.0 (Si−CH). − $C_{28}H_{52}N_{60}Si_2Ti$ (592): calcd. C 56.15, H 8.75; N 13.76; found C 56.73, H 8.84, N 14.18.

*Preparation of* **4**: A mixture of **3** (1.39 g, 2.34 mmol) and ε-caprolactam (0.260 g, 2.34 mmol) was dissolved in 30 ml of diethyl ether. The clear solution was stirred for 10 min at 20 °C, stored for 10 h at 4 °C, for another 20 h at −30 °C and finally for 24 h at −78 °C. The mother liquor was decanted off, and the crystals were collected and dried in vacuum. Yield: 1.21 g (1.83 mmol, 78%) of dark red crystals. − $^1$H NMR ($C_6D_6$): δ = 8.19 (d, 2H, *J* = 5.4 Hz, 6-H), 6.11 (s, 2H, 3-H), 6.00 (d, 2H, *J* = 5.4 Hz, 5-H), 3.54 (s, 6H, N−Me), 3.14 (t, 2H, *J* = 4.5 Hz, 7′-H), 2.33 (t, 2H, *J* = 5.3 Hz, 3′-H), 1.85 (s, 6H, APy−Me), 1.44 (s, 14H, Si−*i*-Pr), 1.37−1.31 (m, 16H), 1.23 (m, 2H, 4′-H), 0.96 (m, 2H, 5′-H). − $^{13}$C-NMR ($C_6D_6$): δ = 184.1 (C-2′), 168.9 (C-2), 149.4 (C-4), 140.9 (C-6), 111.2 (C-5), 110.4 (C-4), 48.6, 48.5 (N−Me), 36.2 (C-7′), 31.6 (C-3′), 30.2 (C-6′), 23.5 (C-4′), 21.6 (APy−Me), 19.5 (C-5′), 19.2, 19.0 (CH−Me), 17.0, 16.6 (Si−CH). − $C_{32}H_{56}N_6O_2Si_2Ti$ (661): calcd. C 58.16, H 8.54, N 12.72; found C 56.70, H 8.49, N 12.47.

[1] B. Cornils, W. A. Herrmann (Eds.), *Applied Homogenous Catalysis with Organometallic Compounds*, VCH, Weinheim, Germany, 1996.
[2] A. R. Chakravarty, F. A. Cotton, E. S. Shamshoum, *Inorg. Chim. Acta* **1984**, *86*, 5−11. M. J. Calhorda, M. A. A. F. De C. T. Carrondo, R. Gomes da Costa, A. R. Dias, M. T. L. S. Duarte, M. B. Hursthouse, *J. Organomet. Chem.* **1987**, *320*, 53−62. J. J. H. Edema, S. Gambarotta, A. Meetsma, A. L. Spek, N. Veldman, *Inorg. Chem.* **1991**, *30*, 2062−2066.
[3] R. Kempe, P. Arndt, *Inorg. Chem.* **1996**, *35*, 2644−2649.
[4] R. Kempe, S. Brenner, P. Arndt, *Organometallics* **1996**, *15*, 1071−1074.
[5] M. Oberthür, P. Arndt, R. Kempe, *Chem. Ber.* **1996**, *129*, 1087−1091.
[6] H. Fuhrmann, S. Brenner, P. Arndt, R. Kempe, *Inorg. Chem.* **1996**, *35*, 6742−6745.
[7] A. B. Holmes, C. L. D. Jennings-White, A. H. Schulthess, B. Akinde and D. R. M. Walton, *J. Chem. Soc., Chem. Commun.* **1979**, 840−842.
[8] R. Kempe, A. Spannenberg, S. Brenner, *Z. Krist.* **1996**, *211*, 497−498. R. Kempe, A. Spannenberg, S. Brenner, *Z. Krist.* **1996**, *211*, 499−500. R. Kempe, A. Spannenberg, S. Brenner, *Z. Krist.* **1996**, *211*, 569−570.
[9] QUEST and VISTA statistics of 6 $Zr-C_{sp}$ bonds distances using the Cambridge Crystallographic Data Base.
[10] M. Polamo, M. Leskelä, 2nd Euchem Conference, Como, Italy, 1996.
[11] H. H. Brintzinger, M. H. Prosenc, personal communication.
[12] M. F. Lappert, P. P. Power, A. R. Sanger, R. C. Srivastava, *Metal and Metalloid Amides*, Ellis Norwood Ltd., Chichester, England, 1980.
[13] F. T. Edelmann, *Coord. Chem. Rev.* **1994**, *137*, 403−481.
[14] P. Arndt, C. Lefeber, R. Kempe, A. Tillack, U. Rosenthal, *Chem. Ber.* **1996**, *129*, 1281−1285.
[15] D. Steinborn, R. Taube, *Z. Chem.* **1986**, *26*, 349−359. D. Steinborn, B. Thies, I. Wagner, R. Taube, *Z. Chem.* **1989**, *29*, 333−334. W. A. Nugent, D. W. Ovenall, S. J. Holmes, *Organometallics* **1983**, *2*, 161−162.
[16] G. M. Sheldrick, *Acta Crystallogr. Sect. A* **1990**, *46*, 467−473.
[17] G. M. Sheldrick, University of Göttingen, Germany, 1993.
[96238]